Complex coacervation of pea protein isolate and tragacanth gum: comparative study with commercial polysaccharides.

Jérémy CARPENTIER [a,c], Egle CONFORTO [b], Carine CHAIGNEAU [c], Jean-Eudes VENDEVILLE [c], Thierry MAUGARD [a]

[a] Université de La Rochelle, UMR CNRS 7266, LIENSs, UFR Sciences, Avenue Michel Crépeau, 17042 La Rochelle, FRANCE

[b] Université de La Rochelle, UMR CNRS 7356, LaSIE, UFR Sciences, Avenue Michel Crépeau, 17042 La Rochelle, FRANCE

[c] IDCAPS, filiale R&D INNOV'IA, 4 rue Samuel Champlain, Z.I. Chef de Baie, 17000 La Rochelle, FRANCE

*Author to who correspondence should be addressed

E-mail: thierry.maugard@univ-lr.fr

Phone : +33 5 16 49 82 77

Key Words

Pea Protein Isolate, Tragacanth gum, Complex coacervates, Protein-polysaccharide interaction, Zeta potential, Solubility

Abstract

The ability of pea protein isolates (PPI) to form complex coacervates with tragacanth gum was investigated. The coacervate formation was structurally compared to three other PPI-polysaccharide interaction models: arabic gum and sodium alginate (known to form coacervates with PPI) and tara gum, a galactomannan. The effects of the pH and protein/polysaccharide ratio were mainly investigated using turbidity and zeta potential measurements. Regarding the pH of soluble complex formation, the pH of complex coacervates increased with the increase in protein-anionic polysaccharide mixture ratio. SEM images revealed the ability of the spray-drying process to form spherical particles of pea protein-polysaccharide complexes. The specificity of the microparticle surface was protein-dependent. FTIR analyses of coacervates showed the electrostatic interaction between the PPI and the polysaccharides. The results showed that tragacanth gum could be used as an alternative to gum arabic to form complex coacervates with PPI based on zeta potential measurements and coacervation yield studies.

1. Introduction

For a few years, plant proteins were of a growing interest for ingredient industry as an alternative to animal sources (gelatin, whey, casein) due to safety concerns (Toews and Wang, 2013). Among plant proteins, yellow pea (*Pisum sativum L.*) protein isolates (PPI) represent attractive hydrocolloids in food and nutraceutical applications due to their health benefits, their allergen and gluten-free properties, a wide availability and low price. The composition of pea proteins is mainly comprised of albumin (10-20% of total proteins) and of two major globulin proteins (70-80% of the total proteins): legumin (11S; 350—400kDa), vicilin and convicilin (7S; 150 and 290kDa respectively) (Adebiyi and Aluko, 2011). Pea protein contains a wide range of charged amino acids, especially lysine (≈6%), aspartic acid (≈11%), glutamic acid (≈17%), arginine (≈7%), leucine (≈7%) in its polypeptide chains exhibiting the polyelectrolyte nature of pea proteins (Boye et al., 2010).

The establishment of interaction between proteins and polysaccharides lead to the formation of complexes that can improve the functionalities of proteins to stabilize emulsions and foams (Tamnak et al., 2016), control the structure and texture of foods and biomaterials (Turgeon et al., 2003), or to design carrier vehicles in the protection and delivery of active compounds to targeted sites and improve their bioavailability (Jain et al., 2016).The complex coacervation, also known as an associative phase separation, is characterized by an electrical balance between two oppositely charged polyelectrolytes (such as a protein, polysaccharide) in aqueous media. Two phases are thus obtained: a biopolymer rich phase and a solvent rich phase. This phenomenon depends on the conditions such as the pH, charge density and molecular weight of the related polymers, the colloid concentration, temperature and ionic strength of media, etc. (Turgeon et al., 2003; Weinbreck et al., 2003). Not all polyelectrolytes are subject to this phenomenon. Complex coacervation is a thermodynamic phenomenon that can be driven enthalpically or entropically by driving forces such as electrostatic interactions or counterion release, with contributions from hydrogen bonding and hydrophobic interactions (Kayitmazer, 2017).

Three critical structure-forming events (pH_C, $pH_{\phi1}$, $pH_{\phi2}$) have been defined based on the changes in turbidity curves during the titration from alkaline to acidic pH (Liu et al., 2009). These events correspond to four different phase behaviors: the co-solubility of biopolymers ($pH > pH_C$), the formation of soluble complexes ($pH_c > pH > pH_{\phi1}$), the formation of complex coacervates inducing a strong increase in turbidity ($pH_{\phi1} > pH > pH_{\phi2}$),and the dissolution of complexes due to the protonation of reactive groups on the polysaccharide backbone ($pH < pH_{\phi2}$). A maximum optical density (OD), also called pH_{opt}, takes place between $pH_{\phi1}$ and $pH_{\phi2}$, corresponding to the maximum amount of coacervates produced at the electrical equivalence of the relevant biopolymer. It has been described that from $pH_{\phi1}$ to pH_{opt} the electrostatic attractive forces become stronger, reaching the maximum electrostatic interaction. This event is a key factor for microencapsulation applications (de Vries et al., 2003; Turgeon et al., 2003; Weinbreck et al., 2003). Controlled protein-polysaccharide interactions through complex coacervation improve their functional role as ingredients, without chemical modification (Nesterenko et al., 2012).

Many studies have been focused on the phase behavior of pea protein-polysaccharide complexes, including pea protein - alginate (Klemmer et al., 2012), pea protein - pectin (Tamnak et al., 2016) or pea protein - arabic gum (Liu et al., 2009). To the best of our knowledge, no study has assessed on the formation of complex coacervates of pea proteins and tragacanth gum as an alternative to arabic gum. Tragacanth gum is an exudate of Asian species of *Astragalus* and consists of two fractions: the water-soluble fraction (composed of tragacanthin) and the water-insoluble fraction (bassorin) and

contain a small amount of protein (>4% w/w) (Anderson and Bridgeman, 1985). Tragacanthin, an anionic component, is composed of a chain of α-(1–4)-linked D-galacturonic acid units, some of which being replaced at O-3 by β-D-xylopyranosyl units and some of them being terminated with D-Galactose or L-Fucose. The galacturonic acid content varies from 10 to 30% per weight in dry matter depending on the species (Balaghi et al., 2010). The gum may be used in numerous applications in food, pharmaceutical and cosmetic industries due to its anionic properties making it highly resistant to acid environments (Nazarzadeh Zare et al., 2019). Tragacanth gum, described as a bifunctional emulsifier, showed efficient acidic oil-in-water emulsions properties (Balaghi et al., 2010; Farzi et al., 2013), gelling abilities and high mucoadhesive properties (Nur et al., 2016). Largely studied in biomedical field, tragacanth gum was identified as non-toxic, non-teratogenic, non-carcinogenic and non-mutagenic, and can be suitable in wound dressing (Ghayempour et al., 2016). It has been reported to be "generally recognized as safe" by the US Food and Drug Administration (FDA) since 1961. Using gum tragacanth as a food additive in food preparations is permitted by the FDA Code of Federal Regulations at the concentration of 0.2-1.3%wt. The Scientific committee for Food of the European Community has approved the tragacanth gum as the food additive E-number E413 (Nazarzadeh Zare et al., 2019).

The aim of this study was to investigate the effect of the nature of marketed polysaccharides, especially gum tragacanth, on the mechanisms determining complex coacervation with the total fraction of a marketed PPI and the resulting complexation-induced changes in protein conformation under optimal coacervation conditions. However, identifying the pH range for the formation of complex coacervates in concentrated biopolymer systems in order to understand their phase transition, structural aspects and functional properties depending on the polysaccharide structure is challenging. Research work has mainly been focused on coacervate formation at concentrations less than 0.3% w/v. Studying the formation of complex coacervates at higher protein concentrations promoted the use of pea protein in food products.

In this study, particles of complex coacervates were assembled by preparing mixtures of PPI and different polysaccharides: arabic gum, sodium alginate, tragacanth gum, known as anionic polysaccharides and tara gum, a non-ionic polysaccharide. This work is structured around two axes of the study. The primary objective was to investigate the influence of factors such as the pH and biopolymer ratios on the phase behavior of PPI-polysaccharide complex coacervates, especially pea protein-tragacanth gum, in order to evaluate the physicochemical properties of these coacervates at a concentration of 0.3% (w/v) by turbidimetric analysis, zeta potential measurements and protein solubility determination. The second objective was to study the coacervation yield of concentrated coacervates (concentration of biopolymers > 1% w/v) in order to study the adaptability of the process in the field of microencapsulation. Finally, Fourier transform infrared spectroscopy (FTIR) and scanning electron microscopy (SEM) were used to determine the structure of dried coacervate particles. The ultimate goal of this study would be to develop microcapsule systems of plant origins from the complex coacervates studied.

2. Material and methods

2.1. Materials and chemicals

Pea protein is dominated by two types of globulin storage proteins: legumin (350-400 kDa) and vicilin (150 kDa). Commercially available pea protein isolate (PPI, 80% protein content) in powder form was purchased from Roquette (Nutralys F85M, Lestrem, FRANCE). The product composition was described as: 7% of relative humidity, 80% of proteins, 3% of carbohydrates, 6% of total fat and 4% of

ashes. Arabic gum was kindly supplied by CNI (Rouen, FRANCE). Tragacanth gum CEROTRAG 887 was purchased from C.E. Roeper GmbH (Hamburg, GERMANY). Tara gum is a galactomannan extracted from the endosperm of the seed of tara shrub *Caesalpinia spinosa*. Tara gum was purchased from Starlight Products (Rouen, FRANCE). The gum obtained consisted of ≥ 80% of galactomannan. Alginate presents a linear structure consisting of (β-1,4)-linked mannuronic and α-guluronic acids, and the proportions depend on the source. Sodium alginate (MANUCOL LD) was kindly supplied by FMC Biopolymer (Philadelphia, USA). All chemicals used in this study were sold as reagent grade and purchased from Sigma-Aldrich (Oakville, ON, Canada).

2.2. Preparation of complex coacervates and turbidimetric acid pH titration

Biopolymer stock solutions were prepared by dispersing PPI, sodium alginate (ALG), arabic gum (GAC), tara gum (TARA) and tragacanth gum (TRAG) powders in Milli-Q™ water, followed by stirring at 500 rpm for 2 hours at room temperature (RT:21-22°C). The total fraction of the protein was used for the study. No treatment was applied to separate the fractions. For ALG, TARA and TRAG, the solution was maintained at 45°C to reduce its viscosity and ensure the complete dissolution of the polysaccharide. All solutions were kept overnight at 4°C to facilitate protein solubility and fully hydrate the polysaccharides. All solutions were prepared at a concentration of 0.5% (w/v).

2.3. Turbidimetric analysis

Turbidimetric acid pH titrations of homogeneous and mixed PPI and polysaccharide systems were performed using Liu et al. (2009) methods with several modifications to identify critical structure-forming events (pH_c $pH_{\phi1}$, pH_{opt}, $pH_{\phi2}$) and biopolymer and pH conditions under which the associative phase separation took place.

Turbidity measurements were performed at different ratios (protein-polysaccharide mixture ratios of 1:1, 2:1, 5:1 and 10:1) with a pH range of 7.0-1.5 using a Fluostar Omega microplate reader (BMG Labtech, FRANCE) at 600 nm in 96 well microplates. Measurements were made at room temperature at a total biopolymer concentration of 0.3% (w/v). Briefly, biopolymer mixtures were mixed from stock solutions to achieve the expected total biopolymer concentration (0.3% w/v) (Ghorbani Gorji et al., 2014) and PPI/polysaccharide ratio (1:1, 2:1, 5:1 and 10:1). Turbidimetric titration upon acidification was achieved via the dropwise addition of HCl (with a gradient HCl concentration of 0.05M > pH 3.5; 0.5M > pH2.5; 1M > pH 2.0). For a 10mL solution of mixture, the maximal volume of HCl added was 2,0mL. The conductimetry didn't exceed 20mS.cm-1. If necessary, a dropwise addition of NaOH 0.5M was achieved to reached pH 7.0. Dilution effects and changes in solution conductivity were considered minimal. Structure-forming transitions were measured graphically from the curve according to (Weinbreck et al., 2003), whereas pH_{opt} corresponded to the maximum OD at 600 nm. All measurements were made in triplicate. A homogeneous solution of PPI or polysaccharides (GAC, TRAG, ALG and TARA) were used under the same solvent conditions and at a biopolymer concentration of 0.3% (w/v) to compare the profiles with mixed solutions.

2.4. Protein solubility determination

The pH-dependence of the percentage of protein solubility of the mixture and homogeneous PPI solutions was tested using the Pierce™ BCA protein assay kit (Thermo Scientific). Briefly, 20 µL of standard or a sample from the center of the supernatant of the mixture preparation were added to 200 µL of BCA working reagent in a 96 well microplate. After a 30-second agitation on a plate shaker, the plate was incubated at 37°C for 30 minutes. Then, the plate was cooled to room temperature and the absorbance was measured at 562nm using a Fluostar Omega microplate reader (BMG Labtech, FRANCE). The protein solubility was estimated as:

$$PS = \frac{Protein\ concentration\ of\ supernatant}{Protein\ concentration\ of\ initial\ solution} \times 100$$

2.5. Electrophoretic mobility

The electrophoretic mobility of PPI-GAC, PPI-ALG, PPI-TRAG, PPI-TARA mixtures and homogeneous biopolymer solutions was investigated according to the pH (range: 7.0 - 1.5) using a Zetasizer Nano-ZS90 (Malvern Instruments, Westborough, MA). The solution pH was decreased by 0.5 pH unit increments through the dropwise addition of hydrochloric acid (0.05M > pH7.0; 0.5M > pH 2.5). Samples were prepared as described in the section above to a final biopolymer concentration of 0.3% (w/v). Using the Henry equation, the electrophoretic mobility was used to estimate the zeta potential:

$$UE = \frac{2\varepsilon \times \xi \times f(\kappa\alpha)}{3\eta}$$

Where η is the dispersion viscosity, ε is the permittivity, f(κα) is a function related to the ratio of particle radius (α) and the Debye length (κ). Using the Smoluchowski approximation, f(κα) was equal to 1,5. All measurements were equilibrated at 25°C for 60s and analysed in triplicate.

2.6. Coacervation yield of concentrated mixtures

Mixed solutions were prepared as for the turbidimetric analysis at a total biopolymer concentration of 5.0% (w/v), except for PPI-TRAG and PPI-TARA mixtures at a ratio of 2:1 that were diluted respectively to 2% and 1% (w/v) due to the viscosity of the polysaccharide solutions (Table 1). The pH was adjusted between 2.5 and 4.5 with 0.5M HCl.

Table 1: Total biopolymer concentration of the various mixed Protein-polysaccharides solutions tested

Ratio	PPI-TRAG	PPI-GAC	PPI-ALG	PPI-TARA
2:1	**2% w/v**	5% w/v	5% w/v	**1% w/v**
5:1	5% w/v	5% w/v	5% w/v	5% w/v
10:1	5% w/v	5% w/v	5% w/v	5% w/v

Briefly, the mixture was left for 60 minutes at room temperature, followed by centrifugation at 1,000 g for 10 minutes. The volume of supernatant was recovered, and the weight of the resulting pellet after drying at 105°C in oven and supernatant was recorded. The coacervate yield was calculated as:

$$CY = \frac{Dry\ weight\ of\ coacervates}{Total\ weight\ of\ protein, polysaccharides\ used\ in\ the\ preparation} \times 100$$

The protein solubility of the mixtures was also determined using the same procedure as described above.

2.7. Preparation of particles

The spray-drying technology was used to prepare microparticles from feed solutions, composed of pea protein – polysaccharide complex coacervates. The solutions were prepared as follows: an amount of PPI and polysaccharide (arabic gum, sodium alginate, tragacanth gum and tara gum) powders was dissolved separately in distilled water by stirring at 500 rpm for 2 hours at room temperature. For ALG, TARA and TRAG, the solution was maintained at 45°C to reduce the viscosity of solution and ensure the complete dissolution of the polysaccharide.

Then the solutions of proteins and polysaccharides were mixed at a protein/polysaccharide ratio of 5:1, and the pH was adjusted to the previously determined optimal value. The feed solutions were

dried in a Mini Spray Dryer Büchi 190 (Büchi Laboratory Equipment, Switzerland), inlet air temperature at 140°C and outlet at 80°C, nozzle of 0.7 mm, and 0,4 Lh^{-1} feed rate. The feed solution was kept under low magnetic stirring at 300 rpm during the drying step. The microparticles were collected from the container, closed hermetically in an opaque packaging and stored at 4°C.

2.8. Fourier transformation infrared (FTIR) spectroscopy study

FTIR spectra of spray-dried complexes and biopolymer powders were recorded using a Spectrum 100 FT-IR spectrometer (Perkin Elmer). Transmission spectra were obtained within a range of 4,000-650cm^{-1} using 32 scans at a resolution of 4 cm^{-1}. The scattering correction procedure was used to correct spectra for the baseline. Mean spectra were calculated from triplicate of independent measurements.

2.9. ESEM morphological observations

The surface morphology of the samples was monitored using an environmental scanning electron microscope (ESEM) (QUANTA 200 Environmental Field Effect Gun apparatus, FEI, FRANCE). The observations were made according to Conforto et al. (2015) with several changes. The particles were deposited on conductive carbon double-faced adhesive tape on aluminum SEM stubs. As described by the author, no coating was applied to the samples before the observation in order to avoid any alteration of the particle surface. The analyses were performed in environmental mode under water vapor pressure with a beam current between 0.1 and 2 nA and an accelerating voltage in the 11-20 kV range. Secondary electron (SE) images were obtained using a Large-Field (LFD) detector. Details of the surface morphology were obtained by varying the water vapor pressure within the 1.20-1.30 mbar range as well as the accelerating voltage of the primary beam.

2.10. Statistical analysis

All measurements were carried out at least in triplicate using freshly prepared samples and data were reported as mean and standard deviation.

3. Results and discussion

3.1. Investigation of the protein-polysaccharide interaction by optical density measurement

The effect of the pH 7.00-1.50) and biopolymer mixture ratio (1:1 – 10:1) on the complex formation were investigated in admixtures of PPI and separately four different polysaccharides (ALG, GAC, TRAG and TARA) at a constant total biopolymer concentration of 0.3% (w/v) by OD measurements. A comparative study was shown in **figure 1A** for the 2:1 ratio of each PPI-polysaccharide mixture. OD curves of the mixture supernatant compared to the OD of the homogeneous protein solution are shown in **Figure 7 (supplemental data)**.

The homogeneous PPI system has been described in the literature as a bell-shaped turbidity curve according to the pH, where OD starts to increase at a pH of about 6.50 and reaches a maximum OD between pH 3.30 and 4.30, where a flattening of the curve top occurs, related to protein self-aggregation. OD decreases at pH 1.70 (Klemmer et al., 2012). **(Figure 1A)**.

The absorbance of PPI-TRAG mixtures revealed a different profile from that of PPI and TRAG homogeneous solutions alone, suggesting an interaction between the protein and the polysaccharide. **(Figure 7A)**. The turbidity of a homogeneous tragacanth gum solution did not change as a function of pH as confirmed by the literature (Ghorbani Gorji et al., 2014; Jain et al., 2016). Mixed PPI-TRAG complexes at a ratio of 2:1 formed at pH 5.54 (referred to as pH_c), leading to a slight increase in OD under acidification (**Figure 1A**). Interactions between PPI and TRAG are assumed to

take place between the negative charges of the carboxylic acid groups of TRAG chains and the positively charged patches on PPI surface. The presence of TRAG caused a shift in turbidity curves towards lower pH values compared to PPI alone by reducing the PPI-PPI aggregation. The pH_c became ratio-independent for ratio ranging between 1:1 and 10:1 (**Figure 7A**). With further acidification, the complexes with a ratio of 2:1 tended to grow at pH 4.94, resulting in the formation of insoluble complexes (referred to the second critical pH parameter $pH_{\phi 1}$). At this point, the OD strongly increased, switching from a transparent to a cloudy dispersion (**Figure 1C**). It increased curvilinearly and a shift of $pH_{\phi 1}$ value was observed with the increase in mixture ratio from pH 4.80-5.10 at a ratio of 1:1 to pH 6.30-6.70 at the mixture ratio of 10:1 (**Figure 7A**)(Lan et al., 2020). This phenomenon was attributed to the rise of self-PPI aggregates formation by increasing the protein concentration in the biopolymer mixture. The turbidity further increased until reaching a maximum OD at pH_{opt} (pH 4.54). At this pH value, an overall charge neutralization was supposed to occur in the biopolymer mixture. At pH_{opt}, the mixtures contained the maximum amount of coacervates and thus showed the maximum OD. Then, a decreasing of OD occurred with further acidification. As for $pH_{\phi 1}$, pH_{opt} increased with the increase in mixture ratio. Overall, a shift of coacervation events towards higher pHs was observed as the biopolymer mixture ratio increased (pH 4.49 at a ratio of 1:1 to pH 4.92 at a ratio of 10:1) **(Figure 1B)**. As the same way, it was observed that pH_c, $pH_{\phi 1}$ and $pH_{\phi 2}$ also increased with mixture ratio from 1:1 to 10:1 (respectively from 6.0 to 7.0 for the pH_c value, from 5.0 to 6.5 for the $pH_{\phi 1}$ value and 2.5 to 4.0 for the $pH_{\phi 2}$ value). At a PPI-TRAG ratio of 1:1, the charges of TRAG chains are supposed to saturate the charges of pea proteins. As the mixture ratio increased, the proteins were in excess, resulting in an increased amount of PPI-PPI aggregates and less complex formation, as previously reported in a PPI-GA interaction study (Liu et al., 2009). A dissolution of the electrostatic complexes at $pH_{\phi 2}$ occurred when the electrostatic attractive forces declined between the macromolecules due to the protonation of acid functions of TRAG (pH 1.50-2.50). All complexes were assumed to be dissolved near pH 2.04 as revealed by the absence of OD. The dissolution pH was independent of the mixture ratio.

The formation of soluble and insoluble complexes occurred at a PPI-GAC mixture ratio of 2:1 at pH 4.50 and 4.05, respectively (**Figure 1A**). The increase in turbidity continued up to pH 3.49 reaching the maximal OD value. This value corresponded to the optimal pH value for the maximum formation of PPI-GAC complexes. At $pH_{\phi 2}$ (2.97), the OD decreased because of the dissociation of the formed complexes. This dissociation would be explained by the protonation of carboxylic acid groups, preventing the association with amino groups of proteins due to electrostatic interactions. Together with the increase in biopolymer ratio, a shift of the optimal pH value was observed. This event was explained by the increase in NH_3^+/COO^- ratio in the protein/polysaccharide mixture. The maximum OD for pH_{opt} was obtained at a ratio of 2:1. It could be assumed that it corresponded to the optimal ratio/pH_{opt} couple for the maximum formation of PPI-GAC complexes obtained (**Figure 7B**). The results are in accordance with other studies (Liu et al., 2009). A shift of pH_{opt} was also observed towards higher pH values with the increase in mixture ratio from 1:1 to 10:1 (**Figure 1B**).

In PPI-ALG mixture at a ratio of 2:1, the critical events attributed to the formation of soluble and insoluble complexes were identified at pH 5.59 (pH_C) and 4.04 ($pH_{\phi 1}$), respectively, and the optimal biopolymer interactions occurred at pH 2.96 (pH_{opt}) **(Figure 1A)**. Together with the increase in biopolymer mixture ratio, the critical pH values shifted towards higher pHs (**Figure 1B**). A strong decrease in OD at $pH < pH_{opt}$ was observed, indicating the occurrence of a partial dissolution of the formed complexes. The maximum OD at pH_{opt} increased from 0.15 at a PPI-ALG ratio of 1:1 to 0.48 at a PPI-ALG ratio of 5:1 (**Figure 7C**). By comparing the different ratios, the 5:1 ratio showed the maximum OD at pH_{opt} value. It suggests that this ratio was considered as the optimal condition to the production complex coacervates from PPI -ALG couple.

Overall, the pH_{opt} increased progressively with the increase in mixture ratio for the case of polyanionic polysaccharide. According to the literature, pH_{opt} values increase with the mixture ratio until a maximum value is reached after which the OD reached a plateau with further increases in biopolymer mixture ratio (Klemmer et al., 2012).

Regarding PPI-TARA mixtures, the critical events associated with the formation of complex coacervates were identified only at ratios of 1:1 and 2:1 **(Figure 1A, 7D)**. The optimal biopolymer interaction occurred at pH 4.48 and 3.58, respectively. Regarding the evolution of pH_{opt}, a shift of pH_{opt} was observed in **Figure 1B**. The behavior was different from other protein-polysaccharide mixtures, as the pH_{opt} decreased with the increase of PPI-TARA ratio. As the ratios increased from 5:1, the turbidity profile of PPI-TARA mixtures was similar to that of homogeneous PPI. Although the latter ratios presented a profile similar to that of PPI alone, the OD of the profile decreased with increasing mixture ratios. For example, for ratios of 5:1 and 10:1 ratios and homogenous PPI at pH 5.50, the OD was respectively of 0.295, 0.157, and 0.088. This observation suggests an increase in protein solubility in the presence of tara gum.

The magnitude of the increase was dependent on the nature of the polysaccharide involved and the mixture ratio. Comparing gum tragacanth, gum arabic and sodium alginate, it seemed that the pH_{opt} decreased with the negative net charge of the polysaccharide. Previous studies have shown that the pH tends to plateau at higher biopolymer ratios (Klemmer et al., 2012).

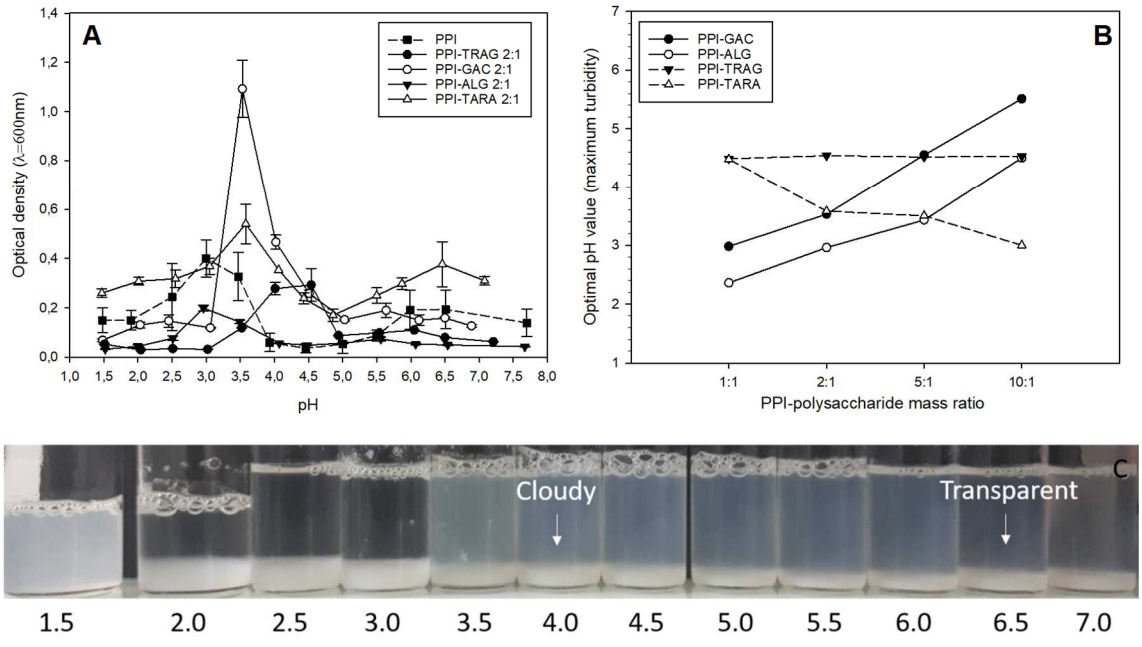

Figure 1: A) Curves of the mean turbidity of PPI-TRAG, PPI-GAC, PPI-ALG and PPI-TARA mixtures at a 2:1 ratio according to the pH. B) Critical pH value (pH_{opt}) according to the mass ratio of mixtures of PPI and different polysaccharides (GAC, ALG, TRAG, TARA).C) Appearance of PPI-TRAG at a 2:1 mixing ratio as a function of pH.

3.2. Zeta potential

The zeta potential analysis allows an understanding of the formation and stability of coacervates formed by electrostatic interactions between oppositely charged proteins and polysaccharides. Changes in zeta potential were investigated according to the pH during the same acid titration as the turbidity profile (pH 7.0-2.0), and according to mixture ratio (1:1-10:1).

PPI showed a cationic nature at pH values less than 4.80 because of the protonation of the amino groups ($-NH_3^+$, theoric pKa of about 9.4) while it had an anionic nature at pH values greater than 4.8 due to the deprotonation of carboxyl groups (COO^-, theoric pKa of about 2.5 to 4.5) (Jones and McClements, 2010) **(Figure 2A**). It was admitted that the pka could change locally depending on the structure of the protein. The isoelectric point (IEP; pI) of commercial pea globulins is known to be in the 4.5-5 pH range, which is consistent with our values (Adebiyi and Aluko, 2011; Cuevas-Bernardino et al., 2018).

Tragacanth gum, arabic gum and sodium alginate showed a negative zeta potential, the absolute value of which increased as the pH increased **(Figure 2A)**. Like for other anionic biopolymer, the deprotonation of carboxylic groups occurred with the increasing of pH. At higher pH values, the zeta potential no longer changed.

Tragacanth gum, like arabic gum, showed a relatively strong polyelectrolyte behavior with a maximum zeta potential of -28,5 mV at pH > 5.0 and approached a neutral zeta potential at pH < 2.0 (ZP= -2.7 mV). Structurally, the major fraction of Arabic gum (89% of the total; 280 kDa) consists of a β-(1-3)-galactopyranose backbone highly branched with β-(1-6)-galactopyranose residues terminating in arabinose and glucuronic acid and/or 4-O-methyl-glucuronic acid units (i.e. carboxylic groups from glucuronic acid units) only at the terminus of each branch). This provides the arabinogalactan with its anionic nature. Arabic gum is known to contain about 15-16% of glucuronic acid units (Osman et al., 1993).

Tragacanth gum consisted in two fractions: the water-soluble fraction (composed of tragacanthin) and the water insoluble fraction (composed of bassorin). Tragacanthin, a pectic component, is composed of a chain of α-(1–4)-linked D-galacturonic acid units, some of which being replaced at O-3 by β-D-xylopyranosyl units and some of them being terminated with D-Galactose or L-Fucose. Bassorin is reported as a neutral, highly branched arabinogalactan (of type II) comprising (1–6)- and (1–3)- linked core chains containing galactose and arabinose (both in the form of furanose and pyranose) and side groups of (1–2)-, (1–3)- and (1–5)-linked arabinose units occurring as monosaccharides or oligosaccharides (Kora and Arunachalam, 2012).The galacturonic acid content varies from 10 to 30% per weight in dry matter depending on the species (Balaghi et al., 2011).

Tara gum had a low negative zeta potential between -8 and 0 mV for the pH range tested **(Figure 2A)**. The absence of ionisable (acidic or basic) groups allowed the gum to maintain neutrality, and therefore a pKa value estimate was not applicable. Tara gum, unlike most types of anionic polysaccharides (pectin, carrageenan, etc…), is considered a non-ionic polysaccharide. The main chain of the structure consists of β-(1,4)-mannose units with galactose with α-(1,6)-linked branches with a mannose-to-galactose ratio of 3:1 (Barbosa et al., 2019). Its structure is mainly composed of hydroxyl groups, resulting in its neutral nature. It has been demonstrated that other gums such as Guar, Konjac, locust bean gums, also known as gluco- and galactomannans, have the same profile (Barbosa et al., 2019).

Sodium alginate showed the highest negative value of zeta potential. Manucol LD (the commercial sodium alginate used) has been described by Horniblow et al. as a sodium alginate with a molecular weight of 145 kDa and a galacturonic acid - mannuronic acid ratio of 38:62 (Horniblow et al., 2016). Thus, alginate possesses larger carboxylic acid extremities, explaining the higher maximum zeta

potential values compared to arabic gum and tragacanth gum, due to differences in their polymeric structures.

A charge neutralization could be assumed since the addition of anionic polysaccharides is known to induce to cationic protein adsorption via an electrostatic attraction at pH 3.00-3.50.

Regarding PPI-TRAG mixtures, all mixture ratios showed intermediate zeta potentials between those of the two separate biopolymers in solution **(Figure 2B)**. As the net charge of biopolymer mixture is closed to zero, the formation of complex coacervation occurred.

Therefore, the IEP was used to represent the pH at which the zero net charge of a biopolymer mixture was achieved, and the influence of biopolymer mixture ratios on the IEP is shown in **Figure 2B, C, D, E.** The electrophoretic mobility corresponded to the mean of electrophoretic mobility of unbound PPI and polysaccharides and that of PPI-polysaccharide complex coacervates. At a mixture ratio of 1:1, the electrophoretic mobility obtained from PPI-TRAG mixture was different from the isoelectric point of PPI alone, decreasing from pH 4,8 (PPI alone) to 3,0 (PPI-TRAG mixture). The mixture showed surface charges similar to those of TRAG with zeta potentials remaining negative within the pH range of 7.0-3.0. As the mixture ratio increased, the isoelectric point changed towards higher pH values, reaching a pH value of 4.20 at a mixture ratio of 10:1, close to homogeneous PPI solution **(Figure 2F)**. Similar results have been reported for the association of tragacanth gum with whey proteins (Raoufi et al., 2016). Moreover, a high zeta potential magnitude of soluble complexes, observed at pH > 4.50, has highlighted an electrostatic repulsion in the system, preventing protein precipitation (Klassen and Nickerson, 2012).

The electrophoretic mobility of the PPI-GAC mixture at a ratio of 1:1 was electrophoretically neutral at pH 3.00 **(Figure 2C)**. Electrophoretic mobility measurements of the PPI-GAC mixture at a ratio of 2:1 allowed estimating the net neutral surface charge of the formed complexes at pH 3.49, which was consistent with the pH_{opt} of the system. Data were in accordance with similar studies of PPI-GAC complexes (Liu et al., 2009). At a higher pH, the formed complexes carried a net negative charge when the charge contribution from GA was superior to that of PPI. In contrast, at a lower pH, a net positive charge of the complexes was found when the positive charge contribution from PPI dominated due to the protonation of glucuronic acid residues of GA., the IEP of the mixture shifted with a trend similar to PPI-TRAG mixtures when the mixture ratio increased towards higher pH values **(Figure 2F)**.

The addition of ALG to PPI shifted the pH of the net neutrality from 4.80 (homogeneous PPI) to 1.47 at a PPI-ALG ratio of 1:1 **(Figure 2D)**. As shown by Klemmer et al., an electrophoretic mobility profile similar to that of the homogeneous ALG solution was identified, and a negative charge was retained within the examined pH range (Klemmer et al., 2012). The increased protein content in the mixture ratio inducing a shift towards higher pHs (**Figure 2F**). The pHs of the net neutrality were close to pH_{opt} values at a corresponding biopolymer mixture ratio, suggesting that at pHs close to pH_{opt}, charge neutralisation occurred.

In contrast, the pH corresponding to the net neutrality did not shift with the addition of TARA regardless of the mixture ratio **(Figure 2E, F)**. The pH of the net neutrality was equivalent to 4.50 in all mixture ratios. The maximum zeta potential value increased with the ratio, due to the increasing addition of proteins, which were charged, to the mixture. Thus, the evolution of the zeta potential in this mixture was mainly due to the amount of PPI added to the mixture.

The Charge neutralization can be modulated by altering the charge of one or both biopolymers or by varying the mixture ratios between PPI and polysaccharides. The zeta potential values obtained were

due to the contribution of complex coacervates but also to unbound PPI and polysaccharides that greatly contribute to the measured net charge according to the ratio and the excess of one of the biopolymers in the mixtures. In all mixture ratios, the zeta potential value of dispersions became more positive with the decrease in pH from 7.00 to 2.00, suggesting the formation of more positively charged complexes. For all mixtures, complexes carried a net negative charge at pH>pI, whereas at pH<pI, the complexes carried a net positive charge.

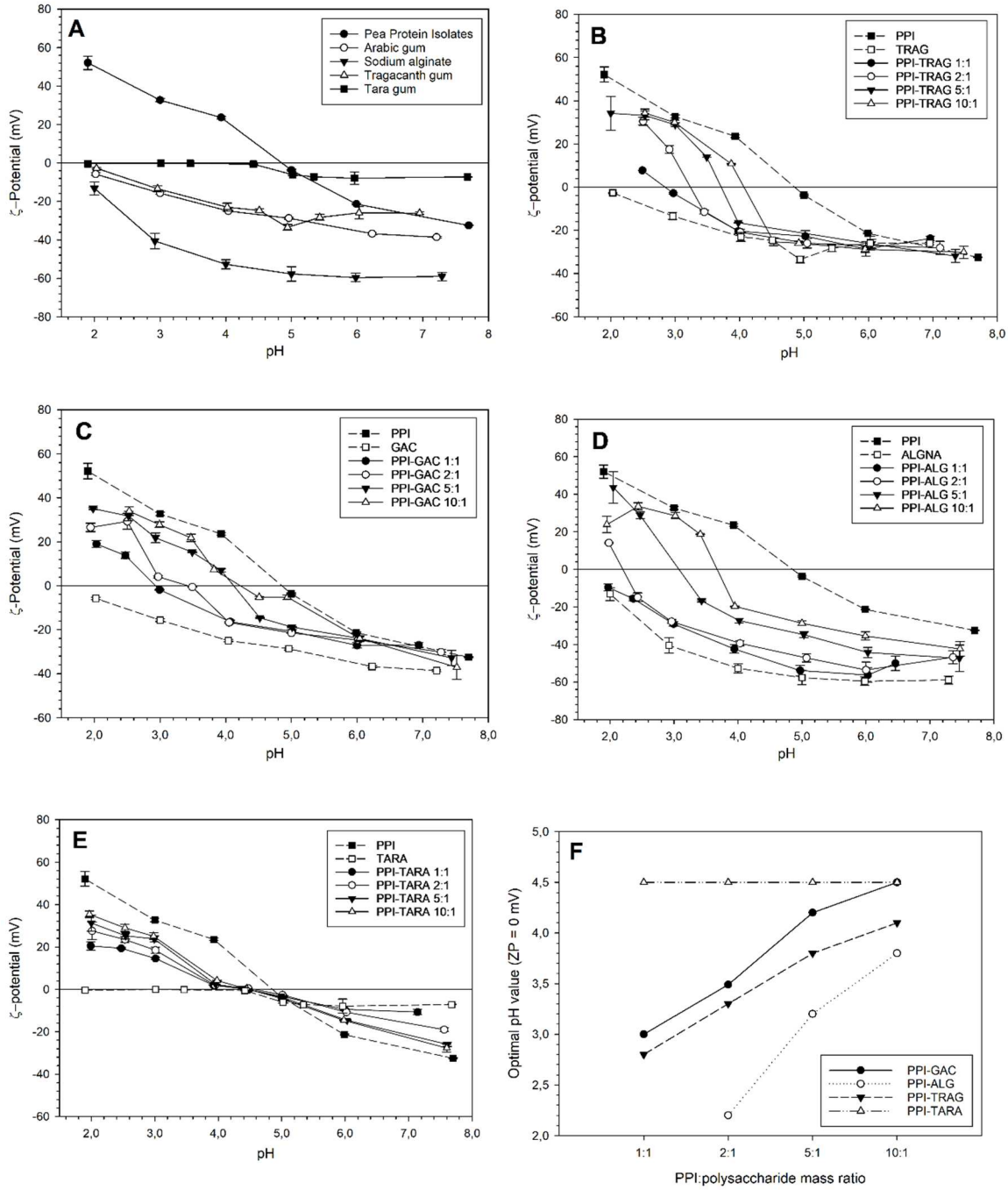

*Figure 2: Mean zeta potential (mV) of pea protein isolates and polysaccharides (arabic gum, sodium alginate, tragacanth gum and tara gum) (**A**) and mixtures (PPI-TRAG (**B**), PPI-GAC (**C**), PPI-ALG (**D**) and PPI-TARA (**E**))at different ratios according to the pH. Data represents the mean ± standard deviation (n=3). **F**) Critical pH values according to the mass ratio of PPI and different polysaccharides (GAC, ALG, TRAG, TARA).*

3.3. Pea protein solubility

In this section, the pH-dependent solubility profile of the soluble PPI-polysaccharide complexes formed was explored.

The PPI solubility profile showed a downward trend with a decrease from 22% at pH 7.00 to its minimum (3%) at pH 4.5, corresponding to the protein IEP **(Figure 3A)**. It was followed by an increase in solubility with progressive pH decreases. Similar protein solubility profiles have been reported with commercial PPI (Guo et al., 2019).

Regarding PPI-TRAG mixtures, the presence of TRAG increased the PPI protein solubility at pH 4.50 (pI) from 2.5% (homogeneous PPI) to 14.6% (PPI-TRAG ratio of 2:1) **(Figure 3A)**. This trend was explained by the decrease of PPI self-aggregation with addition of tragacanth gum. This has also been reported for pea protein - pectin mixtures ((Warnakulasuriya et al., 2018). Also, the pH for PPI minimum solubility was shifted from 4.50 to 3.50 as the PPI-TRAG mixture ratio decreased from 10:1 to 2:1. This phenomenon was in agreement with the previously observed phase behavior. This has previously been demonstrated by the protein-polysaccharide complexes formation at pH less than 4.00, increasing protein solubility in an acid pH range (Guo et al., 2019).

Similarly, the addition of GAC and ALG to PPI mixed systems induced a shift in the minimum solubility from PPI alone (**Figure 3B, C**). It has been suggested that this shift could linked to soluble and insoluble complexes formation (Liu et al., 2010). Also, a shift of pH range from which a minimal solubility occurred has been observed towards more acidic pHs as the polysaccharide amount increased in soy protein-carrageenan complexes (Molina Ortiz et al., 2004). The addition of ALG to PPI resulted in a loss of solubility at PPI-ALG ratio of 5:1 and 10:1 (0,15 and 0,07% respectively), because protein precipitation dominated in the system. Overall, the complexation with anionic polysaccharides appears to shift the pH of the minimum protein solubility towards more acid pH values (Guo et al., 2019; Klassen et al., 2011; Liu et al., 2010). PPI-GAC and PPI-TRAG mixtures shared a similar trend in pH-dependent protein solubility profile in terms of pH value shifting **(Figure 3E)**. Differences observed between the PPI-ALG, PPI-GAC and PPI-TRAG mixtures could be related to the charge of the polysaccharide (Klassen et al., 2011). As reported by Klassen *et al.*, alginate and carrageenan differ in their surface charge, leading to a difference in canola protein precipitation, ι-carrageenan being more likely to induce canola protein precipitation (Klassen et al., 2011). Similarly, the tendency of polysaccharides tested in this study to form complexes with PPI was dependent on the surface charge of polysaccharides, with alginate > arabic gum > tragacanth gum.

Regarding PPI-TARA mixtures, since TARA is a non-ionic polysaccharide, the association with PPI plays a minor role. The incompatibility observed was directly correlated with the protein self-association as observed at ratios ranging between 5:1 and 10:1, because they had a profile similar to that of homogeneous PPI **(Figure 3D)**. As the PPI-polysaccharide ratio decreased, the protein solubility increased for values greater than or less than pI by limiting PPI self-aggregation. As showed in **Figure 3E,** the minimum solubility at the different PPI-TARA ratios was close to the pI of PPI because the biopolymers were not charged at this pH. Overall, it has been admitted that the pH and ionic strength only affect protein self-association in protein - non-ionic polysaccharide systems (Syrbe et al., 1998).

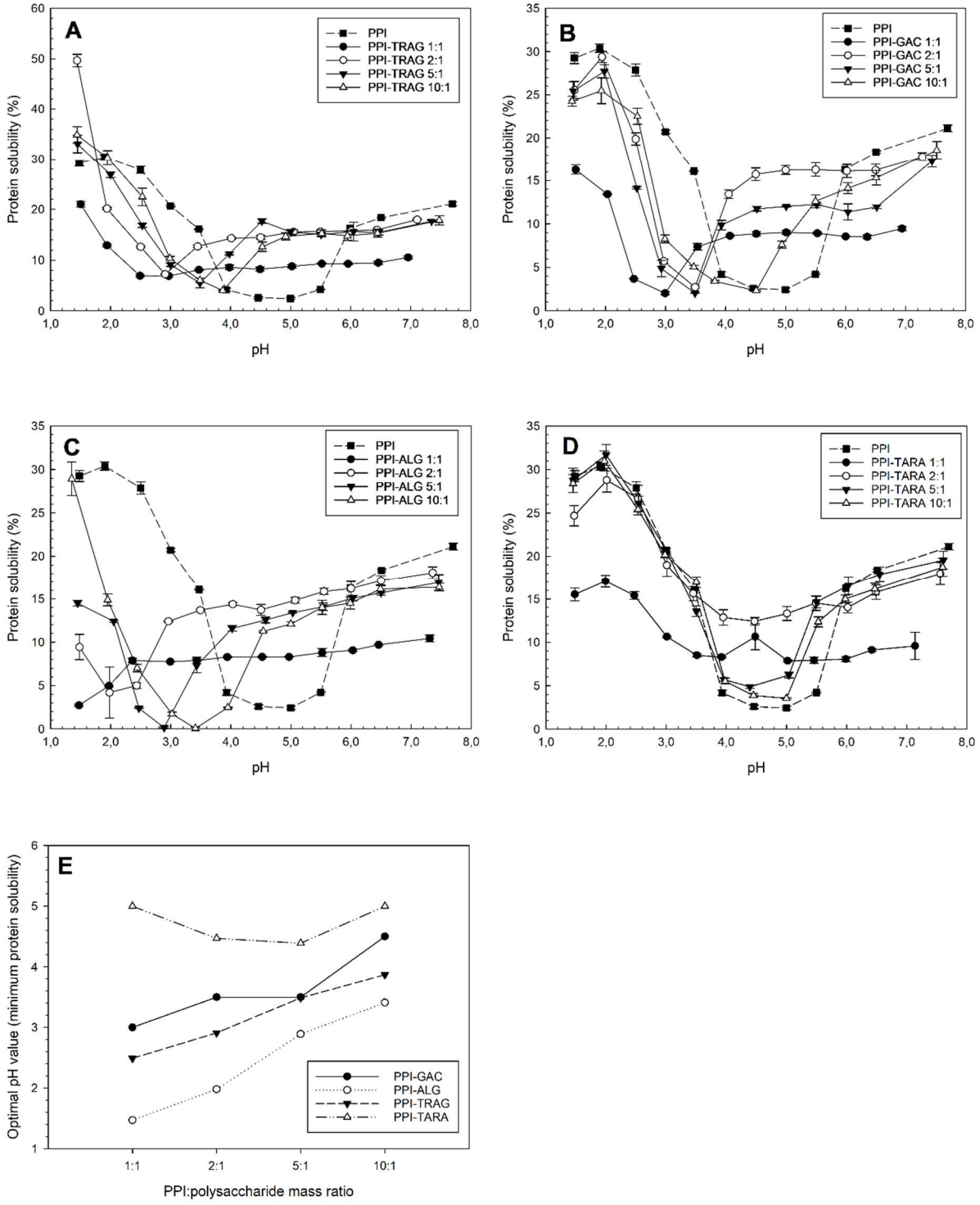

*Figure 3: Percentage of protein solubility of the PPI-TRAG (**A**), PPI-GAC (**B**), PPI-ALG (**C**) and PPI-TARA (**D**) mixtures at different ratios according to the pH. Data represents the mean ± standard deviation (n=3). **E**) Critical pH values according to the mass ratio of mixtures PPI and different polysaccharides (GAC, ALG, TRAG, TARA) corresponding to the minimum protein solubility.*

3.4. Coacervation yield of concentrated mixtures

PPI-TARA and PPI-TRAG mixtures were prepared at a total biopolymer concentration of 1.0% and 2.0% (w/v), respectively, due to the high viscosity of the gums, while PPI-GAC and PPI-ALG mixtures were prepared at a concentration of 5.0%. The coacervation yield was obtained from the percentage

of protein solubility measured in the supernatant after centrifugation. The coacervation yield was mainly associated with complex coacervation between the pea proteins and the polysaccharides and with the self-aggregation of pea proteins.

The yields obtained in the PPI-GAC mixtures were in agreement with the previously performed analyses (turbidity and zeta potential) **(Figure 4B)**. The maximum yield corresponded to a mixture ratio of 2:1 at pH 3.50, which was in agreement with the higher OD value obtained in the turbidity analysis. A pH shift was also observed as the mixture ratio increased. However, this shift was not clearly identified as in 0.3% total biopolymer study since the yields seemed to be very close to one another and the maximum yield value obtained did not seem significant.

Similarly, in the PPI-ALG and PPI-TRAG mixtures, the best yields obtained were respectively for the ratio of 5:1 at pH= 3.50 and for the ratio of 2:1 at pH= 3.0 **(Figure 4A, C)**. A shift was also observed as previously reported. However, the results of the PPI-TRAG mixtures differed from those of the turbidity analysis by 0.50 pH unit. The yield was improved in the presence of alginate due to its higher surface charge, compared to PPI-TRAG and PPI-GAC mixtures. In all pea protein - polysaccharide mixtures, the pH value corresponding to maximal value yield shifted towards higher pHs. This shift of pH values was similar to the pH shift limit in the turbidity and zeta potential studies, showing that the pH required for the maximum production of coacervates shifted as the pea protein - anionic polysaccharide mixture ratio increased.

In contrast, the coacervation yield obtained for PPI-TARA mixtures seemed to correspond to a PPI self-aggregation mechanism as tara gum was considered as a non-ionic polysaccharide **(Figure 4D)**. The presence of TARA appeared to decrease the aggregation, since the solubility increased (or the obtained yield decreased).

The higher yield obtained with independent ratios corresponded to the neutral net charge value obtained in the zeta potential analysis. Differences in maximal complex coacervation yield values obtained between PPI-anionic polysaccharides could be due to the polysaccharide surface charge (alginate > arabic gum > tragacanth gum) as observed in the previous protein solubility study.

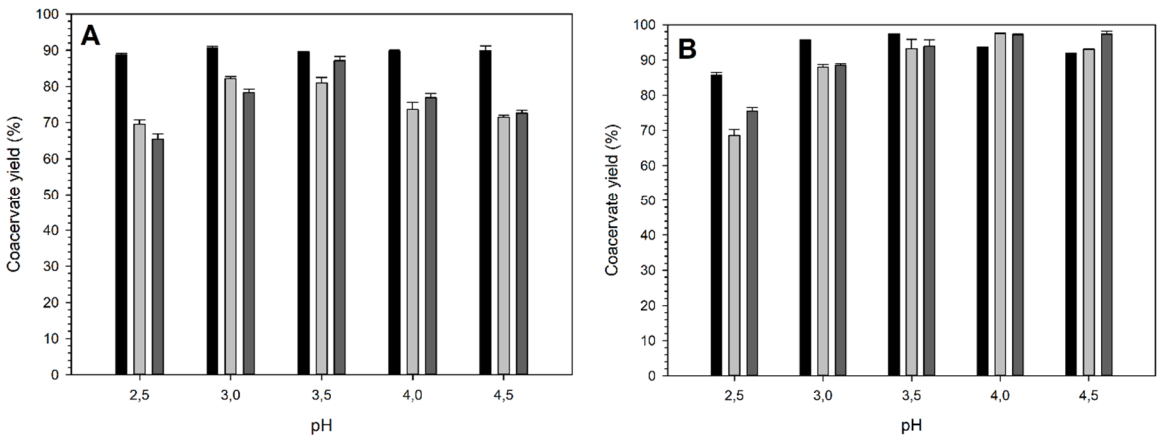

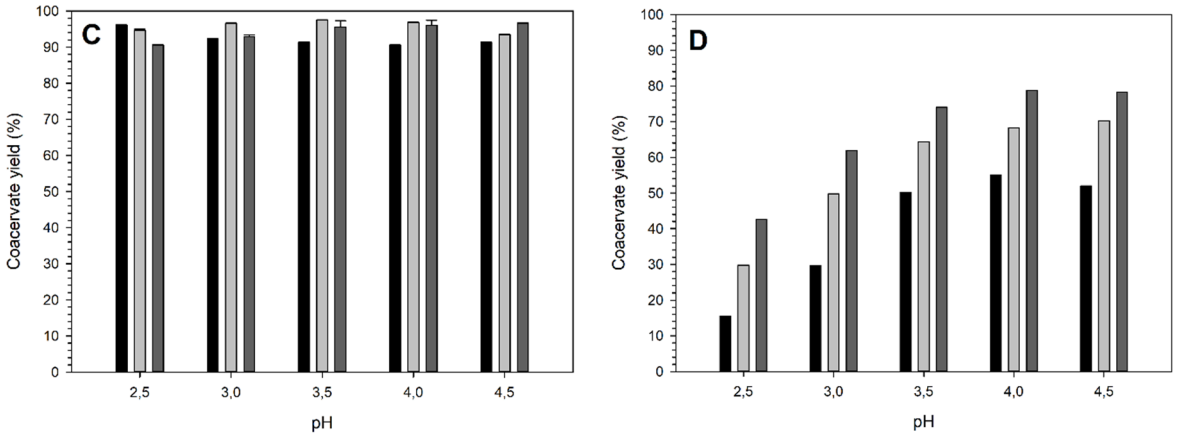

Figure 4: Coacervation yield of pea protein – polysaccharide mixtures (PPI-TRAG (A), PPI-GAC (B), PPI-ALG (C) and PPI-TARA (D)) at ratios of 2:1 (black), 5:1 (light grey) and 10:1 (dark grey) determined based on the protein solubility in concentrated solutions.

3.5. FTIR analysis

Previously prepared complex coacervates were spray-dried to obtain microparticles. Then, they were characterized by FTIR and observed by SEM.

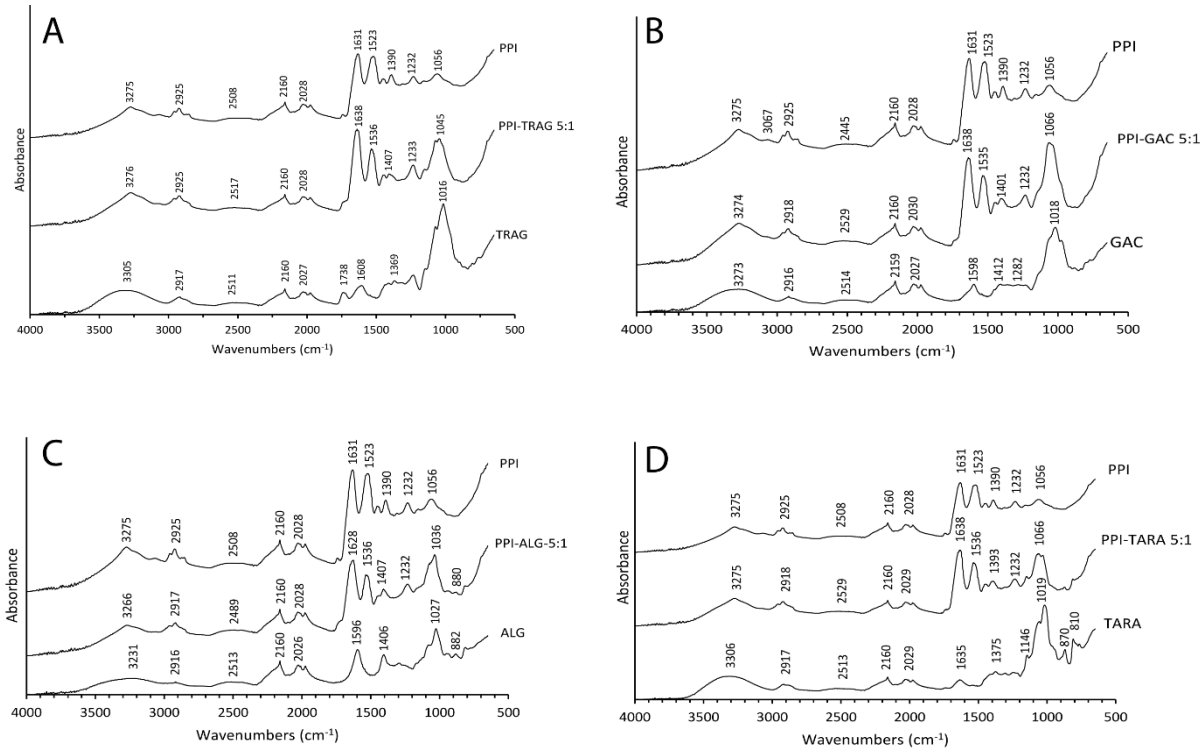

Figure 5: FTIR spectra of the PPI-TRAG (a), PPI-GAC (b), PPI-ALG (c) and PPI-TARA (d) mixtures prepared at PPI: Polysaccharide ratio of 5 :1.

The FTIR analysis provides information on the structure of proteins and polysaccharides and their interactions in the mixture. Molecularly, the interactions of functional groups can lead to the appearance of new bands and to changes in absorption band or location in the FTIR spectra. **Figure 5** shows the FTIR spectra of raw materials as well as the dried protein-polysaccharide mixtures.

Regarding the tragacanth gum spectrum, the broad band at 3305 cm^{-1} could be attributed to stretching vibrations of hydroxyl- groups in the gum **(Figure 5A)**. The bands at 2800-3000 cm^{-1} corresponded to asymmetric and symmetric stretching vibrations of C-H groups. The broad band at 2160 cm^{-1} was related to the carbonyl species of the gum. The peak at 1608 cm^{-1} could be attributed to the characteristic asymmetrical stretching of carboxylate group. The symmetrical stretching of carboxylate groups could be associated with the bands present in the zone of 1369 cm^{-1} (Kora and Arunachalam, 2012). The peaks of the region of 1016 cm^{-1} were associated with the fingerprint region of carbohydrates.

The spectrum of arabic gum showed an absorption band at 3290-3305 cm^{-1} corresponding to -OH hydrogen bonded groups, characteristics of glucosidic rings **(Figure 5B)**. The peak at 2916 cm^{-1} was due to the presence of sugars, galactose, arabinose, rhamnose, alkane with C-H stretching and aldehyde C-H. The peaks at 1598 and 1412 cm^{-1} were respectively related to COO- symmetric and asymmetric stretching. The peak at 1018 cm^{-1} was associated with alkene C-H bends (Daoub et al., 2018).

The spectrum of sodium alginate showed characteristic bands corresponding to carboxylic, ether and hydroxyl groups **(Figure 5C)**. The peak at 1406 and 1596 cm^{-1} were attributed to symmetric and asymmetric $-COO^-$ stretching vibration, while the peak at 3231 cm^{-1} was related to the stretching vibration of -OH groups (Nayak and Pal, 2011).

The spectrum of tara gum showed characteristic peaks at 810 and 870 cm^{-1}, which are associated with the presence of α-D-galactopyranose units and β-D-mannopyranose units (**Figure 5D)**. The peaks at 1019 and 1146 cm^{-1} corresponded to the C-O stretching vibration of pyranose rings. (Figueiro et al., 2004). The peak at 1375 cm^{-1} was attributed to $-CH_2$ and C-OH symmetrical deformations. The peak at 1635 cm^{-1} was associated with the association with water. The broad peaks ranging from 2800 to 3000 cm^{-1} were related to the O-H and C-H stretching vibration.

Regarding pea proteins, a strong -OH contraction vibration band and a C-H stretching band were respectively observed at 3275 cm^{-1} and 2925cm^{-1} **(Figure 5)**. The stretching or bending of C=O at 1631 cm^{-1}, N-H deformation and C-N stretching at 1523 cm^{1} and C-N stretching at 1232 cm^{-1} corresponded to amide I (high content of β-sheet structures), II and III, respectively (Aguilar-Vázquez et al., 2018). The peak of amide I was due to a high content of β-sheet structures (Wang et al., 2011). The peak at 1056 cm^{-1} corresponded to C-O vibration stretching.

Regarding the spectra of raw materials and coacervates, the functional groups present in the coacervates closely resembled the functional groups of pea proteins and the polysaccharides involved. The domination of PPI structure was clearly established in the spectrum of PPI-TRAG complexes due to the higher protein ratio (5:1), but it was different from that of each individual biopolymer.

Regarding PPI-TRAG complexes, the peaks corresponded to amide I of PPI shifted from 1631 to 1638 cm^{-1} **(Figure 5A)**. The peaks related to amide II and III were shifted respectively from 1523 and 1232 cm^{-1} to 1536 and 1233 cm^{-1}. The shifting of amide peaks could be explained by conformational changes in α-helix structures towards β-sheets configuration (Mousazadeh et al., 2018). Moreover, a decrease of the intensity of amide II and III peaks (respectively at 1536 cm^{-1} and 1407 cm^{-1}) was observed in the complexes compared to the separate pea protein solution due to a decrease of free functional groups. The disappearance of peaks corresponding to TRAG, especially at 1635 cm^{-1}, could also point out the presence of interactions between the two biopolymers (Mousazadeh et al., 2018). In addition, the disappearance of the peak might be attributed to the excess of protein in the mixture. The "fingerprint region" of PPI-TRAG coacervates showed a broad band (1100-950 cm^{-1}) which could be due to the superposition of PPI (1056cm^{-1} corresponding to carboxylate stretching vibration) and TRAG (peak 1073 and 1016cm^{-1}, C-O-C stretching vibration) spectra. This involved the establishment of electrostatic interactions between pea proteins and the gum leading to the formation of coacervates.

596 Overall, the carbonyl-amide region was affected during the formation complex coacervates. The
597 coacervates did not show the symmetric -COO^- stretching vibrations (1608 cm^{-1}) found for TRAG. A shift of
598 wavenumbers was observed in amide peaks towards higher values compared to native PPI and could be
599 explained by the establishment of electrostatic interactions between the amino groups of PPI and the
600 carboxylic groups of TRAG. This phenomenon have also been observed in gelatin-carboxymethylcellulose
601 complex formation (Duhoranimana et al., 2017) . The same observations were made for PPI-GAC mixture.
602 In the case of PPI-ALG mixture, a shift of the amide I peak wavenumber was observed towards lower value
603 compared to native PPI (1631 cm^{-1} to 1628 cm^{-1}).

604

605 **3.6. ESEM observations**

606 A systematic examination of the surface morphology of the spray-dried microparticles was achieved by
607 Environmental Scanning Electron Microscopy (ESEM) **(Figure 6)**. The average size of microparticles ranged
608 between 2 and 10µm. The aggregation of sub-micron particles on larger particles was observed. The
609 microparticles showed a predominantly spherical shape with a rough surface and concavities. These
610 wrinkles/distorsions have been attributed to the uneven shrinkage of the particles during the drying
611 process with rapid evaporation of water (Eratte et al., 2015; Sheu and Rosenberg, 1998). The appearance of
612 these microstructures has been observed by various authors in the preparation of microparticles using a
613 spray-drying process (Gharsallaoui et al., 2010; Nesterenko et al., 2012; Pierucci et al., 2007). These
614 wrinkles could improve the release properties of microparticles due to a greater surface area. Details of the
615 microparticle surface showed a regular polymeric network, without any porous structure, suggesting a high
616 integrity of the encapsulating materials. However, some nanometric irregularities were observed at the
617 surface of some particles, also modulating the release of potential encapsulated compounds (Jun-xia et al.,
618 2011) (**Figure 6**, PPI-TRAG x100,000). These irregularities could be described as a network composed of
619 organized “fibrillar-like” strands of 25-75 nm. These nanostructures are similar to those observed during
620 pea protein gelation in the presence of calcium chloride (Munialo et al., 2014). However, the morphology of
621 pea protein-based particles obtained using spray-drying process has not been clearly described in the
622 literature at a nanometric scale since the use of a coating during SEM observations could cover the
623 roughness and porosities on the particle surface due to their small dimensions. The metal-coated particle
624 surface looked smoother than it actually was (Conforto et al., 2015). Since this roughness was found on the
625 various protein-polysaccharide mixtures, it could be assumed that it could be linked with the nature of the
626 protein instead of the nature of the polysaccharide.

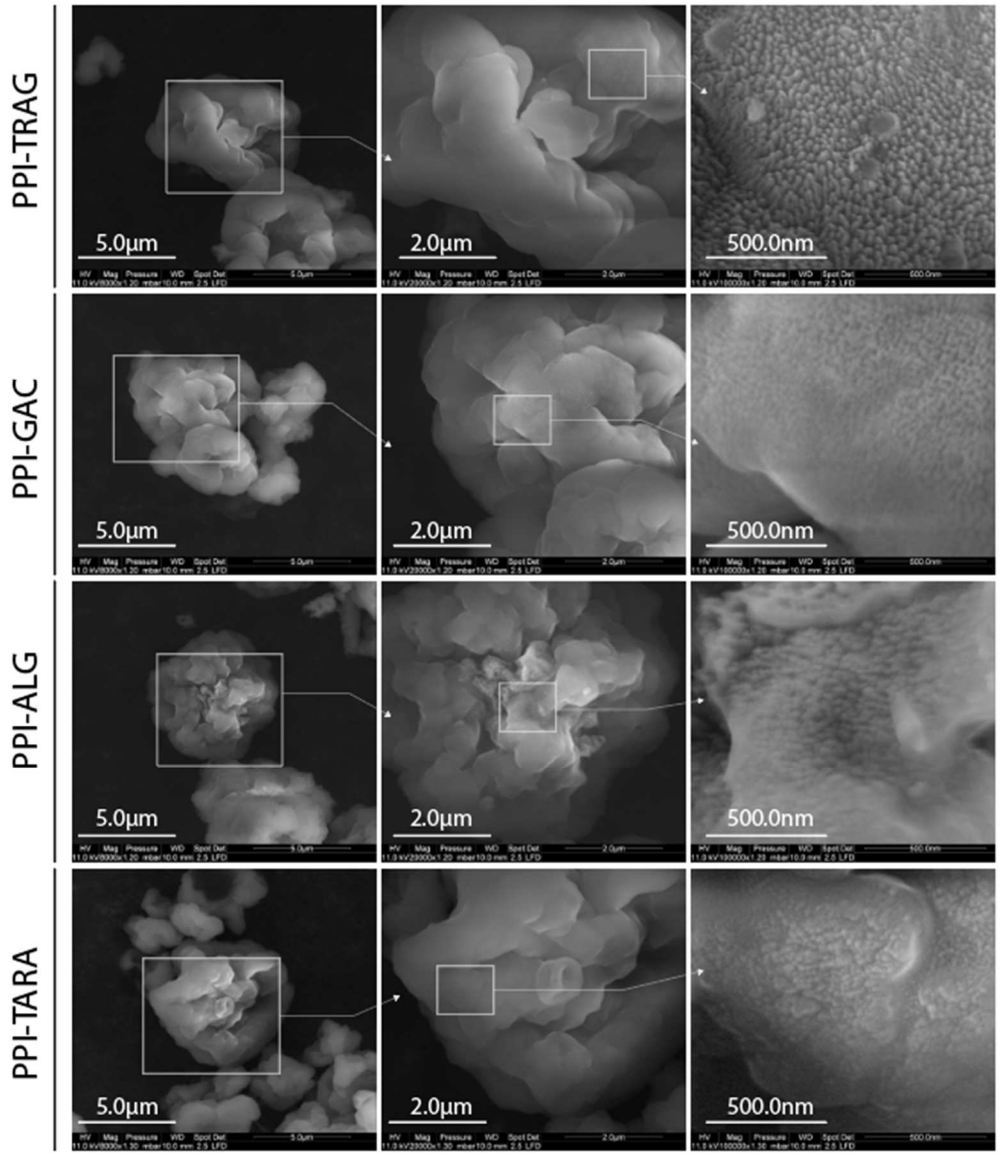

627

628 *Figure 6: SEM observations (left to right: x8,000; x20,000; x100,000) of spray-dried PPI-TRAG, PPI-GAC , PPI-ALG and PPI-*
629 *TARA coacervates prepared at a ratio of 5:1.*

630 ## 4. **Conclusion**

631 This study compared the ability of commercial tragacanth gum to form complex coacervates with pea
632 proteins to three other polysaccharides: arabic gum, sodium alginate and tara gum. Tragacanth gum, arabic
633 gum and sodium alginate formed effectively complex coacervates with PPI. Complex coacervation is highly
634 dependent on the pH as well as the nature and concentration of the polysaccharide used. This study
635 showed the optimum parameters for complex coacervation between the pea protein and tragacanth gum
636 with a maximum interaction at a PPI/TRAG ratio of 2:1 at pH 4.5. The zeta potential analysis, that allowed
637 performing the preformulation study, identified a pH shifting from 2.8 to 4.0 as the PPI-TRAG mixture ratio
638 increased from 1:1 to 10:1. Overall, the pH values of critical structure-forming events, especially pH_{opt}
639 values, were shifted towards higher pHs as the protein content increased in all PPI-polysaccharide mixtures.
640 Moreover, the pH-dependent protein solubility profile was shifted towards more acid pH values as the
641 biopolymer ratio decreased. For more concentrated solutions, there was a correspondence of pH values
642 between optimal yield and the neutral net charge value obtained in the zeta potential analysis of 0.3% w/v
643 solutions. Differences in yield obtained could be due to the polysaccharide surface charge (alginate > arabic

gum > tragacanth gum). Compared to arabic gum, tragacanth gum appears to be a good alternative since its properties are similar in association with PPI. Regarding PPI-TARA mixtures, the possible formed complexes were dependent on pea protein self-aggregation since tara gum was considered a non-ionic polysaccharide. The electrostatic interaction between proteins and polysaccharide backbones were verified by FTIR. The surface morphology of the generated microparticles was studied by SEM. The spray-dried microparticles maintained a spherical shape and a surface without fracture. An observation at nanometric scale showed fibrillar-like structures which could be of interest to further studies in other fields of coacervation. Based on our findings, PPI associated with different anionic polysaccharides could be used in the area of microencapsulation.

Declaration of competing interest

The authors are not aware of any affiliations, memberships, funding or financial holdings that could affect the objectivity of this article.

Acknowledgements

We thank Dr Egle Conforto from the CCA platform of La Rochelle University for her assistance in SEM observation. This work was financially supported by INNOV'IA and IDCAPS (La Rochelle, France).

5. References

Adebiyi, A.P., Aluko, R.E., 2011. Functional properties of protein fractions obtained from commercial yellow field pea (*Pisum sativum L.*) seed protein isolate. Food Chemistry 128, 902–908.

Aguilar-Vázquez, G., Loarca-Piña, G., Figueroa-Cárdenas, J.D., Mendoza, S., 2018. Electrospun fibers from blends of pea (Pisum sativum) protein and pullulan. Food Hydrocoll. 83, 173–181.Anderson, D.M.W., Bridgeman, M.M.E., 1985. The composition of the proteinaceous polysaccharides exuded by astragalus microcephalus, A. Gummifer and A. Kurdicus—The sources of turkish gum tragacanth. Phytochemistry 24, 2301–2304.

Aryee, F.N.A., Nickerson, M.T., 2012. Formation of electrostatic complexes involving mixtures of lentil protein isolates and gum Arabic polysaccharides. Food Research International 48, 520–527.

Balaghi, S., Mohammadifar, M.A., Zargaraan, A., 2010. Physicochemical and Rheological Characterization of Gum Tragacanth Exudates from Six Species of Iranian Astragalus. Food Biophysics 5, 59–71.

Balaghi, S., Mohammadifar, M.A., Zargaraan, A., Gavlighi, H.A., Mohammadi, M., 2011. Compositional analysis and rheological characterization of gum tragacanth exudates from six species of Iranian Astragalus. Food Hydrocolloids 25, 1775–1784.

Barbosa, J.A.C., Abdelsadig, M.S.E., Conway, B.R., Merchant, H.A., 2019. Using zeta potential to study the ionisation behaviour of polymers employed in modified-release dosage forms and estimating their pKa. International Journal of Pharmaceutics: X 1, 100024.

Boye, J., Zare, F., Pletch, A., 2010. Pulse proteins: Processing, characterization, functional properties and applications in food and feed. Food Res. Int. 43, 414–431.

Conforto, E., Joguet, N., Buisson, P., Vendeville, J.-E., Chaigneau, C., Maugard, T., 2015. An optimized methodology to analyze biopolymer capsules by environmental scanning electron microscopy. Materials Science and Engineering: C 47, 357–366.

Daoub, R.M.A., Elmubarak, A.H., Misran, M., Hassan, E.A., Osman, M.E., 2018. Characterization and functional properties of some natural Acacia gums. Journal of the Saudi Society of Agricultural Sciences 17, 241–249.

Ducel, V., Richard, J., Saulnier, P., Popineau, Y., Boury, F., 2004. Evidence and characterization of complex coacervates containing plant proteins: application to the microencapsulation of oil droplets. Colloids and Surfaces A: Physicochemical and Engineering Aspects 232, 239–247.

Duhoranimana, E., Karangwa, E., Lai, L., Xu, X., Yu, J., Xia, S., Zhang, X., Muhoza, B., Habinshuti, I., 2017. Effect of sodium carboxymethyl cellulose on complex coacervates formation with gelatin: Coacervates characterization, stabilization and formation mechanism. Food Hydrocolloids 69, 111–120.

Figueiro, S., Goes, J., Moreira, R., Sombra, A., 2004. On the physico-chemical and dielectric properties of glutaraldehyde crosslinked galactomannan–collagen films. Carbohydrate Polymers 56, 313–320.

Gharsallaoui, A., Saurel, R., Chambin, O., Cases, E., Voilley, A., Cayot, P., 2010. Utilisation of pectin coating to enhance spray-dry stability of pea protein-stabilised oil-in-water emulsions. Food Chemistry, 5th Conference on Water in Food 122, 447–454.

Ghayempour, S., Montazer, M., Mahmoudi Rad, M., 2016. Encapsulation of Aloe Vera extract into natural Tragacanth Gum as a novel green wound healing product. International Journal of Biological Macromolecules 93, 344–349.

Ghorbani Gorji, S., Ghorbani Gorji, E., Mohammadifar, M.A., Zargaraan, A., 2014. Complexation of sodium caseinate with gum tragacanth: Effect of various species and rheology of coacervates. International Journal of Biological Macromolecules 67, 503–511.

Guo, Q., Su, J., Yuan, F., Mao, L., Gao, Y., 2019. Preparation, characterization and stability of pea protein isolate and propylene glycol alginate soluble complexes. LWT – Food Science and Technology 101, 476–482.

Horniblow, R.D., Latunde-Dada, G.O., Harding, S.E., Schneider, M., Almutairi, F.M., Sahni, M., Bhatti, A., Ludwig, C., Norton, I.T., Iqbal, T.H., Tselepis, C., 2016. The chelation of colonic luminal iron by a unique sodium alginate for the improvement of gastrointestinal health. Mol. Nutr. Food Res. 60, 2098–2108.

Jain, A., Thakur, D., Ghoshal, G., Katare, O.P., Shivhare, U.S., 2016. Characterization of microcapsulated β-carotene formed by complex coacervation using casein and gum tragacanth. International Journal of Biological Macromolecules 87, 101–113.

Jones, O.G., McClements, D.J., 2010. Functional Biopolymer Particles: Design, Fabrication, and Applications. Comprehensive Reviews in Food Science and Food Safety 9, 374–397.

Kayitmazer, A.B., 2017. Thermodynamics of complex coacervation. Adv. Colloid Interface Sci. 239, 169–177.

Klassen, D.R., Elmer, C.M., Nickerson, M.T., 2011. Associative phase separation involving canola protein isolate with both sulphated and carboxylated polysaccharides. Food Chemistry 126, 1094–1101.

Klassen, D.R., Nickerson, M.T., 2012. Effect of pH on the formation of electrostatic complexes within admixtures of partially purified pea proteins (legumin and vicilin) and gum Arabic polysaccharides. Food Research International 46, 167–176.

Klemmer, K.J., Waldner, L., Stone, A., Low, N.H., Nickerson, M.T., 2012. Complex coacervation of pea protein isolate and alginate polysaccharides. Food Chemistry 130, 710–715.

Kora, A.J., Arunachalam, J., 2012. Green Fabrication of Silver Nanoparticles by Gum Tragacanth (Astragalus gummifer): A Dual Functional Reductant and Stabilizer. Journal of Nanomaterials 2012, 1–8.

Lan, Y., Ohm, J.-B., Chen, B., Rao, J., 2020. Phase behavior and complex coacervation of concentrated pea protein isolate-beet pectin solution. Food Chem. 307, 125536.

Liu, S., Elmer, C., Low, N.H., Nickerson, M.T., 2010. Effect of pH on the functional behaviour of pea protein isolate–gum Arabic complexes. Food Research International 43, 489–495.

Liu, S., Low, N.H., Nickerson, M.T., 2009. Effect of pH, Salt, and Biopolymer Ratio on the Formation of Pea Protein Isolate−Gum Arabic Complexes. J. Agric. Food Chem. 57, 1521–1526.

Molina Ortiz, S.E., Puppo, M.C., Wagner, J.R., 2004. Relationship between structural changes and functional properties of soy protein isolates–carrageenan systems. Food Hydrocolloids 18, 1045–1053.

Mousazadeh, M., Mousavi, M., Askari, G., Kiani, H., Adt, I., Gharsallaoui, A., 2018. Thermodynamic and physiochemical insights into chickpea protein-Persian gum interactions and environmental effects. International Journal of Biological Macromolecules 119, 1052–1058.

Munialo, C.D., van der Linden, E., de Jongh, H.H.J., 2014. The ability to store energy in pea protein gels is set by network dimensions smaller than 50nm. Food Research International 64, 482–491.

Nayak, A.K., Pal, D., 2011. Development of pH-sensitive tamarind seed polysaccharide–alginate composite beads for controlled diclofenac sodium delivery using response surface methodology. International Journal of Biological Macromolecules 49, 784–793.

Nazarzadeh Zare, E., Makvandi, P., Tay, F.R., 2019. Recent progress in the industrial and biomedical applications of tragacanth gum: A review. Carbohydrate Polymers 212, 450–467.

Nesterenko, A., Alric, I., Silvestre, F., Durrieu, V., 2012. Influence of soy protein's structural modifications on their microencapsulation properties: α-Tocopherol microparticle preparation. Food Research International 48, 387–396.

Nur, M., Ramchandran, L., Vasiljevic, T., 2016. Tragacanth as an oral peptide and protein delivery carrier: Characterization and mucoadhesion. Carbohydrate Polymers 143, 223–230.

Osman, M.E., Williams, P.A., Menzies, A.R., Phillips, G.O., 1993. Characterization of commercial samples of gum arabic. J. Agric. Food Chem. 41, 71–77.

Pierucci, A.P.T.R., Andrade, L.R., Farina, M., Pedrosa, C., Rocha-Leão, M.H.M., 2007. Comparison of alpha-tocopherol microparticles produced with different wall materials: pea protein a new interesting alternative. J Microencapsul 24, 201–213.

760 Raoufi, N., Kadkhodaee, R., Phillips, G.O., Fang, Y., Najafi, M.N., 2016. Characterisation of whey
761 protein isolate-gum tragacanth electrostatic interactions in aqueous solutions. Int J Food Sci Technol
762 51, 1220–1227.

763 Sheu, T.-Y., Rosenberg, M., 1998. Microstructure of Microcapsules Consisting of Whey Proteins and
764 Carbohydrates. J Food Science 63, 491–494.

765 Syrbe, A., Bauer, W.J., Klostermeyer, H., 1998. Polymer Science Concepts in Dairy Systems—an
766 Overview of Milk Protein and Food Hydrocolloid Interaction. International Dairy Journal 8, 179–193.

767 Tamnak, S., Mirhosseini, H., Tan, C.P., Tabatabaee Amid, B., Kazemi, M., Hedayatnia, S., 2016.
768 Encapsulation properties, release behavior and physicochemical characteristics of water-in-oil-in-
769 water (W/O/W) emulsion stabilized with pectin–pea protein isolate conjugate and Tween 80. Food
770 Hydrocolloids 61, 599–608.

771 Toews, R., Wang, N., 2013. Physicochemical and functional properties of protein concentrates from
772 pulses. Food Research International 52, 445–451.

773 Turgeon, S.L., Beaulieu, M., Schmitt, C., Sanchez, C., 2003. Protein–polysaccharide interactions:
774 phase-ordering kinetics, thermodynamic and structural aspects. Current Opinion in Colloid &
775 Interface Science 8, 401–414.

776 Wang, C., Jiang, L., Wei, D., Li, Y., Sui, X., Wang, Z., Li, D., 2011. Effect of Secondary Structure
777 determined by FTIR Spectra on Surface Hydrophobicity of Soybean Protein Isolate. Procedia Eng. 15,
778 4819–4827.

779 Warnakulasuriya, S., Pillai, P.K.S., Stone, A.K., Nickerson, M.T., 2018. Effect of the degree of
780 esterification and blockiness on the complex coacervation of pea protein isolate and commercial
781 pectic polysaccharides. Food Chemistry 264, 180–188.

782 Weinbreck, F., de Vries, R., Schrooyen, P., de Kruif, C.G., 2003. Complex Coacervation of Whey
783 Proteins and Gum Arabic. Biomacromolecules 4, 293–303.